Polymer Journal (2019) 51:559–568
https://doi.org/10.1038/s41428-019-0175-6

ORIGINAL ARTICLE

Mechanical properties of microcellular and nanocellular silicone rubber foams obtained by supercritical carbon dioxide

Bin Xiang[1] · Yalan Jia[1] · Yajie Lei[1] · Fengshun Zhang[1] · Jiangping He[1] · Tao Liu[1] · Shikai Luo[1]

Received: 29 October 2018 / Revised: 10 January 2019 / Accepted: 11 January 2019 / Published online: 21 February 2019

Abstract

In this work, nanocellular silicone rubber foams were first prepared by supercritical carbon dioxide. The cellular morphologies and mechanical properties of the microcellular and nanocellular silicone rubber foams are presented. The cell size and cell density of the microcellular silicone rubber foams can reach 1–4 μm and 10^{11} cells/cm^3, respectively. The nanocellular silicone rubber foams have an upper limit diameter of 59 nm, and the density of the nanocellular silicone rubber foams is on the order of 10^{14} cells/cm^3, which is several orders of magnitude greater than that of the typical microcellular silicone rubber foams. The stretching-induced cavitation can play an important role in the formation of the nanocellular structure on cell walls. The effect of the cellular structure on the mechanical properties is investigated. As a result, the nanocellular structure causes an early breakdown, resulting in a decrease in the tensile strength. Furthermore, when the open-cell content (OCC) increases, the compressive curves change from having three regions to two regions, indicating that the compression plateau disappears when the OCC is greater than 0.45.

Introduction

In recent years, foams with an average cell size of less than 1 μm have been regarded as nanocellular foams and have attracted great interest because of the wide range of applications, such as low-*k* materials, filtration membranes, and thermal insulation materials [1, 2]. So far, there have been two methods presented to prepare nanocellular foams [3]. One method is to improve the nucleation number using a heterogeneous nucleation agent [4–6]. For instance, Realinho et al. [4] obtained nanocellular PMMA foams with a cell size of 500 nm through the addition of 2.5 wt% organically modified montmorillonite (oMMT). Zhai et al. [5] found that the cell size of nanocellular polycarbonate foams decreases to 400 nm when nano-silica particles are 9 wt%. The other method is to limit the foaming to a more CO_2-philic phase in the block copolymer [7–9]. For example, Yokoyama et al. [7] prepared PS-PFMA copolymer foams, and the cell size was less than 50 nm. Taki et al. [8] obtained nanocellular foams of PS-b-PMMA copolymer with an average cell size of 40 nm. However, as mentioned, the matrices used to prepare nanocellular foams are all thermoplastic polymers, and previous research has failed to consider the preparation of the nanocellular rubber foams.

A silicone rubber matrix is known to have a large number of silicon–oxygen (Si–O) bonds in the backbone. Si–O bonds have a high bond energy, which is approximately 30% greater than a carbon–carbon bond, causing silicone rubber to have unique properties [10, 11]. Silicone rubber foams not only have the properties of silicone rubber, such as superb chemical resistance, good electrical insulation, high thermal stability, and shape conformity, but also have the characteristics of porous material, such as a low density, sound absorption, and lightweight [12, 13]. Hence, silicone rubber foams have become attractive functional materials and have been widely used in vibration mounts, thermal shielding, press pads and in the aerospace, marine, entertainment, and sporting goods industries [14, 15].

Solvent and chemical foaming methods are the most commonly used methods for the preparation of silicone rubber foams [16, 17]. However, there are many problems with these two methods of preparation, such as low

✉ Tao Liu
liutao_caep@163.com

✉ Shikai Luo
luosk_caep@163.com

[1] Institute of Chemical Materials, China Academy of Engineering Physics, Mianyang 621900, China

preparation efficiency for solvent foaming and environmental pollution for the chemical foaming. In addition, it is difficult to obtain the microcellular or nanocellular morphology of silicone rubber foams when using common methods.

The supercritical foaming method, as a green foaming technology, has been used in the preparation of silicone rubber foams due to its unique properties [18–23]. For example, Hong et al. [18] prepared a microcellular liquid silicone foam with a cellular size of 12 μm. Song et al. [19] first reported that heat vulcanized silicone rubber foams can be prepared with $scCO_2$. Liao et al. [20, 21]. recently reported that the viscoelastic properties of silicone rubber play an important role in the $scCO_2$ foaming process. Yan et al. [22] and Yang et al. [23] prepared silicone rubber foams with a cell size of less than 10 μm and a cell density greater than 10^8 cells/cm^3 by controlling the parameters of the $scCO_2$ foaming. Until now, there have not been investigations that report the preparation of nanocellular silicone rubber foams using $scCO_2$.

Hence, it is our purpose to prepare microcellular and nanocellular silicone rubber foams. In this article, we first exhibit nanocellular silicone rubber foams in the solid-state foaming process. The cellular morphology is adjusted by systematically changing the foaming parameters, such as the silica content, precuring time, and saturation pressure. The relationship between the cellular morphology and mechanical properties of the silicone rubber foams is presented. Furthermore, the formation mechanism of the nanocellular structure will be explained.

Experimental procedure

Materials

Silicone rubber (methyl vinyl silicone with 0.22% vinyl, VMQ 110-2, $Mw = 550{,}000$–$700{,}000$) was provided by Nanjing Dongjue Silicone Group Co., Ltd. (China). Fumed silica (R812S, specific surface area $= 260 \pm 30$ m^2 g^{-1}) was supplied by Evonik-Degussa (Germany). The dicumyl peroxide (DCP) and hydroxyl silicone oil were purchased from Kelong Company (China).

Sample preparation

VMQ, silica, and silicone oil were compounded in the internal mixer (Haake Rheomix 600p) at 105 °C for 15 min, and then, under the same conditions, this compound was re-mixed for 15 min. The silica content was 40, 50, 60, and 70 wt%. Then, 1 g of DCP was added to the compound and mixed for another 15 min at room temperature. Next, the rubber compounds were hot pressed to prepare 2-mm-thick sheets in a vulcanizing press at 130 °C for different times.

Silicone rubber foams were created using the supercritical foaming method. The foaming agent was CO_2. The rubber sheets were placed in a pressure reactor, saturated with supercritical CO_2, and kept at a predetermined temperature and pressure for 1 h. The pressure in the vessel was then released as quickly as possible. After foaming, full curing was performed to maintain the cell structure. The foamed sheet was placed in an air-circulating oven at 160 °C for 30 min and was heat-treated at 190 °C for 1 h. Finally, the density of the silicone rubber foams was calculated by measuring and weighing.

Sample characterization

The silicone rubber mixture was scanned with an RPA2000 rubber process analyzer using a dynamic time sweep. Dynamic time ramp tests were conducted to measure the viscoelastic response of the storage modulus (G') during the curing reaction. The temperature was set to 160 °C, and the frequency was 1 Hz.

Tensile and compressive testing was performed on an RSA G2 solid analyzer in tensile mode. The crosshead rate was set at 0.83 and 0.083 mm/s during the tensile and compressive testing processes, respectively. However, the compressive testing was not carried out with the standard method because the samples were less than 4 mm. The samples were a nonstandard size: a Φ8 mm column with a thickness of approximately 3 mm.

The morphology of the foamed samples was observed using a scanning electron microscope (CamScan Apollo 300). First, the samples were freeze-fractured in liquid nitrogen and then sputter-coated with gold. The cell diameter and cell density were measured using ImageJ software. The cell density (N_f), i.e., number of cells per cubic centimeter of the foams, was calculated by Equation (1) [24]:

$$N_f = \left(\frac{n}{A}\right)^{3/2}\left(\frac{1}{1-V_f}\right) \quad (1)$$

where n is the number of cells on the SEM micrograph, A is the area of the micrograph (cm^2), and V_f is the void fraction of the foamed sample, which can be estimated as

$$V_f = 1 - \frac{\rho_f}{\rho} \quad (2)$$

where ρ and ρ_f are the mass densities of the solid and foamed samples, respectively.

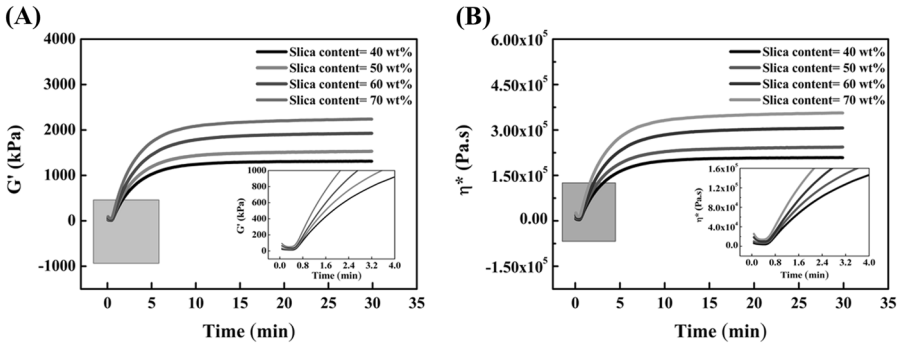

Fig. 1 Curing curves of the silicone rubber composites with various silica contents (**a** storage modulus and **b** viscosity)

Results and discussion

Effect of the silica content on the rheological properties

Figure 1 shows the effect of the silica content on the rheological properties of the silicone rubber composites. Figure 1 has two notable features. First, when the silica content increases from 40 to 70 wt%, G' increases from 1.31 to 2.24 MPa, and η^* increases from 2.08×10^5 to 3.56×10^5 Pa·s. These results mean that the silicone rubber composite with 70 wt% silica has a greater matrix strength compared with that of the silicone rubber composite with 40 wt% silica. The vulcanizing parameters of the silicone rubber composites are shown in Table 1. The scorching time (t_{10}) and optimum cure time (t_{90}) of silicone rubber composites decreased from 0.86 to 0.78 min, and from 8.18 to 7.74 min as the content of silica increased from 40 to 70 phr, respectively. That is, the initial crosslinking is accelerated by the high silica content. Furthermore, with an increase in the silica content, the minimum torque (S'_{min}) and the difference between the maximum torque and minimum torque ($\triangle S'$) of the silicone rubber composites gradually increased.

The matrix strength is known to have an important influence on the foaming process. The greater matrix strength of the silicone rubber can effectively prevent cells from merging and collapsing. Second, one can see that the high content of silica can accelerate the initial crosslinking of the silicone rubber. Hence, the degree of vulcanization of the silicone rubber with the high silica content is greater that of the low silica content rubber given that the curing parameters are the same, and this increase in the degree of vulcanization leads to improvements in the matrix strength. The results given above offer a precondition for the preparation of the nanocellular silicone rubber foams.

Microcellular structure of the silicone rubber foams

Figure 2 shows the cell structure of the microcellular silicone rubber foams. The cell diameter and cell density of the microcellular silicone rubber foams are calculated using Equation (1) according to the SEM micrographs. The cellular properties are illustrated in Fig. 3. The precuring time (t_{pre}) plays a vital role in the cellular morphology because it has an effect on the matrix strength. As t_{pre} increases, the cell diameter decreases, and the cell density increases, as shown in Fig. 3a, b. This result is probably due to the matrix strength of the silicone rubber increasing as t_{pre} increases, which can prevent cells from merging and collapsing. Therefore, a very small cell diameter can be obtained. The same results have also been presented in previous studies [20, 23].

From Fig. 3c, d, when the saturation pressure (P_s) increases, the cell diameter decreases, but the cell density increases. Furthermore, one can see that over the range of the P_s, the influence of the silica content on the cell diameter is not obvious. The cell diameter range is only 2 or 3 μm. In addition, the cell diameter decreases to approximately 1 μm as P_s increases to 22 MPa. However, when the silica content is greater than 60 wt%, P_s has a great influence on the cell density. Compared with that of the low silica content foam, the cell density of the foams with the high silica content increased by more than an order of magnitude and reached 2.83×10^{11} cells/cm^3 when the P_s increased from 16 to 22 MPa. The results can be attributed to two factors. First, silica acts as a nucleating agent; the nucleation energy barrier can be reduced by the addition of the silica, resulting in the provision of a large number of nucleation sites [25]. Second, the nucleation barrier can be significantly decreased when the pressure drop increases [26].

Table 1 The vulcanizing parameters of the silicone rubber composites

Silica content (wt%)	t_{10} (min)	t_{90} (min)	S'_{min} (dNm)	S'_{max} (dNm)	$\triangle S'$ (dNm)
40	0.86	8.18	0.06	12.72	12.66
50	0.84	8.11	0.08	14.9	14.82
60	0.83	7.94	0.11	16.92	16.81
70	0.78	7.74	0.16	19.55	19.39

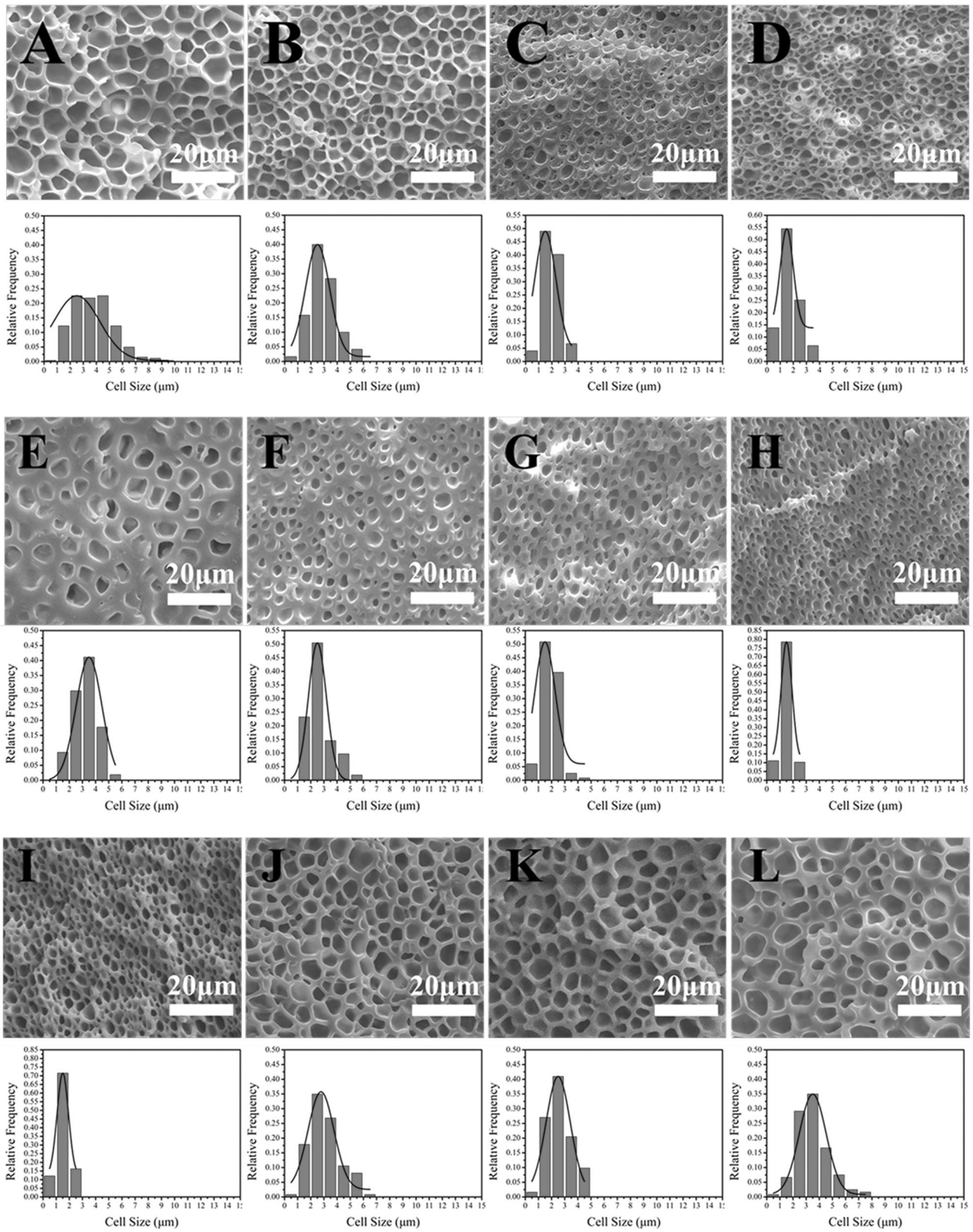

Fig. 2 SEM photographs of the silicone rubber foams: **a–d** the effect of t_{pre} on the cellular morphology ($P_s = 20$ MPa, $T_s = 50$ °C, silica content = 60 wt%); **e–h** the effect of P_s on the cellular morphology ($t_{pre} = 10$ min, $T_s = 50$ °C, silica content = 40 wt%), **i–l** the effect of T_s on the cellular morphology ($t_{pre} = 10$ min, $P_s = 22$ MPa, silica content = 50 wt%)

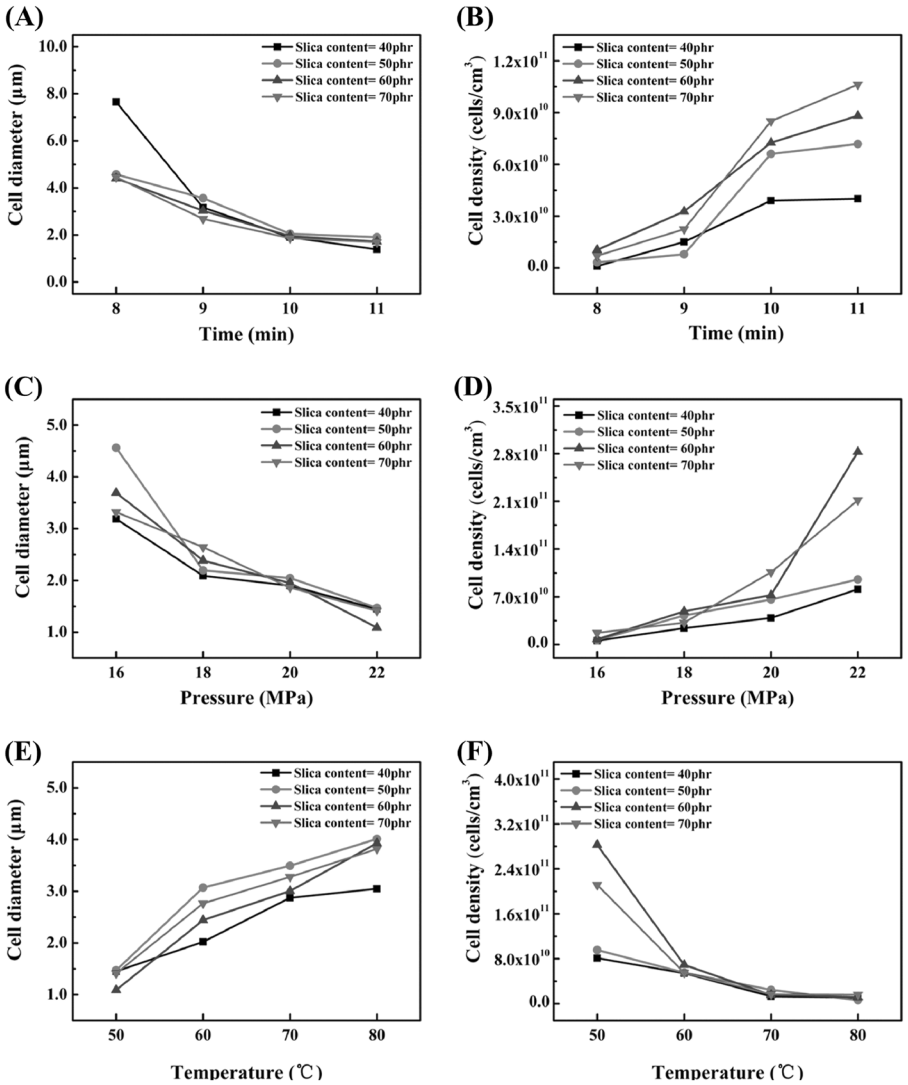

Fig. 3 Cell diameter and cell density of foams with various conditions: **a**, **b** the effect of t_{pre} on the cellular properties (P_s = 20 MPa, T_s = 50 °C, silica content = 60 wt%); **c**, **d** the effect of P_s on the cellular properties (t_{pre} = 10 min, T_s = 50 °C, silica content = 40 wt%); **e**, **f** the effect of T_s on the cellular properties (t_{pre} = 10 min, P_s = 22 MPa, silica content = 50 wt%)

The influence of the saturation temperature (T_s) on the cellular structure is shown in Fig. 3e, f. One can see that the cell diameter increases and the cell density decreases when there is an upward trend in T_s because a high T_s can significantly improve the mobility of the silicone rubber chain and decrease the matrix strength, which leads to coalescing and collapsing [23]. On the other hand, a high T_s will decrease the equilibrium absorbability of CO_2, which results in a reduction in the amount of nucleation [22].

Nanocellular structure of the silicone rubber foams

A nanocellular structure means that the cell size is less than 1 μm. Figure 4 shows the nanoscaled cellular structure that is observed on the cell walls under high magnification. The foams consist of mixed microcellular and nanocellular structure, which are regarded as nano/micro transition foams. This cell structure has been found in some thermoplastic foams [27–30]. However, a mixed microcellular and nanocellular structure was first reported in rubber systems. The reason a nanocellular structure formed could be due to stretching-induced cavitation. The expansion growth of microcells can introduce thermodynamic instability and result in the phase separation of the polymer–gas mixture, which is referred to as stretching-induced cavitation [31]. There are two factors affecting the formation of a nanocellular structure. On the one hand, a large swelling ratio or high cell growth rate can improve the strain energy and result in a nanocellular structure on the cell walls [29]. The silicone rubber matrix is so soft that a large expansion ratio will occur during the foaming process, which is beneficial for producing a nanocellular structure on the cell wall. On the other hand, the cell wall thickness plays a critical role in the formation of the stretching-induced cavitation. A thinner cell wall results in easier cavitation. As the cell walls thin sharply, the cell wall will be penetrated by the cavitation resulting in an open-cell structure occurs. The open-cell content (OCC) is the ratio of the open-cell structure, and the

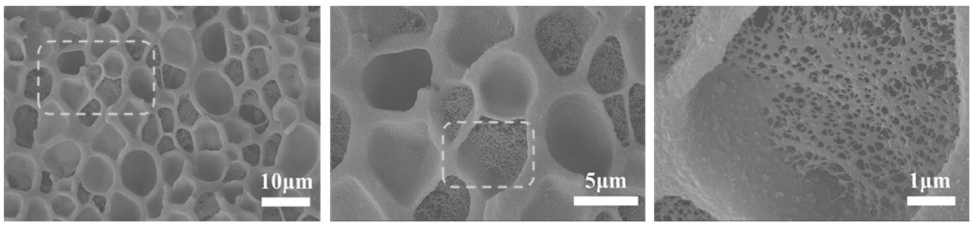

Fig. 4 SEM photographs of the silicone rubber foam with the nanocellular structure

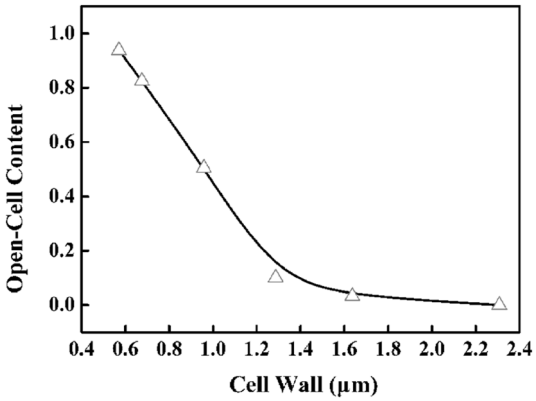

Fig. 5 The effect of the cell wall thickness on the OCC

relationship between the OCC and the cell wall is shown in Fig. 5. When the cell wall thickness is greater than 1.29 μm, the OCC is very low, which indicates that it is difficult to form the nanocellular structure. Furthermore, the OCC increases sharply when the wall thickness is decreased further. The OCC increased by more than 90% when the wall thickness was less than 0.57 μm.

The OCC and cellular properties of the nanocellular foams have been summarized. The contour plot diagram based on all the experimental data is presented in Fig. 6. The silica content, t_{pre} and P_s are the important factors that affect the nanocellular morphology. From Fig. 6a, when the silica content is less than 50 wt%, the OCC is low, and there is no significant change when t_{pre} increases. However, when the silica content and t_{pre} exceed 60 wt% and 9 min, the OCC dramatically improves and even reaches greater than 93%. As shown in Fig. 6b, when the silica content and P_s exceed 60 wt% and 18 MPa, the OCC also sharply improves and could reach greater than 96%. The high OCC is attributed to two factors. First, the high matrix strength can inhibit cells from collapsing, resulting in the formation of a microcellular cell with a high cell density. Second, the high P_s will provide a large number of the nucleation sites, resulting in an increase in the cell density. The cell wall will become thin when the cell density increases. Hence, it is easy to form stretching-induced cavitation, which results in the greater formation of the open-cell structure. From Fig. 6c–f, when the silica content, t_{pre} and P_s increase, the cell diameter decreases and the cell density increases. Additionally, the cell diameter and cell density can reach approximately 59 nm and 6.35×10^{14} cells/cm^3 when the silica content, t_{pre} and P_s are 70 wt%, 11 min, and 22 MPa, respectively. The nanocellular cell structure occurs, and consequently, the cell diameter is much smaller than that of silicone rubber foams made using $scCO_2$ [18–23].

Mechanical properties of the nano/micro silicone rubber foams

Figure 7 schematically shows the stress–strain curves of the nano/micro silicone rubber foams for different foaming parameters. As can be seen, with an increase in the precuring time, the compressive strength of the nano/micro silicone rubber foams increases. When the precuring time of the silicone rubber matrix is greater than 9 min, the curves of the compressive measure for nano/micro silicone rubber foams can be mainly divided into three different regions. First, there is a linear deformation region where the stress linearly increases with the growth of the strain, and the slope is defined as the compressive elastic modulus. Second, a plateau region occurs, indicating that the stress remains constant in the range of the strain. Third, there is a densification region where the stress dramatically increases as the strain increases. However, the stress increases slightly when the strain increases in the plateau region, meaning that the plateau region is not a completely flat plateau. The experimental compressive stress–strain curves of the microcellular foams are consistent with the model proposed for conventional foams by Gibson and Ashby [32]. This indicates that the curves of the nano/micro silicone rubber foams exhibit similar characters as those of conventional foams. According to the morphology of the silicone rubber foams provided above, when the precuring time is greater than 9 min (saturation pressure is 16 MPa), the cellular structure exhibits a continuous honeycomb structure, indicating that an improvement in the strength of the matrix and a reduction of cell size will increase the ability of the cell wall to resist bending. In addition, the cell can provide a longer deformation process in this size, thereby exhibiting a wider compression plateau region in the compressive stress–strain curve. With an increase in the $scCO_2$ saturation pressure, the compressive strength of the nano/micro silicone rubber foams increases, while the width of the compression plate

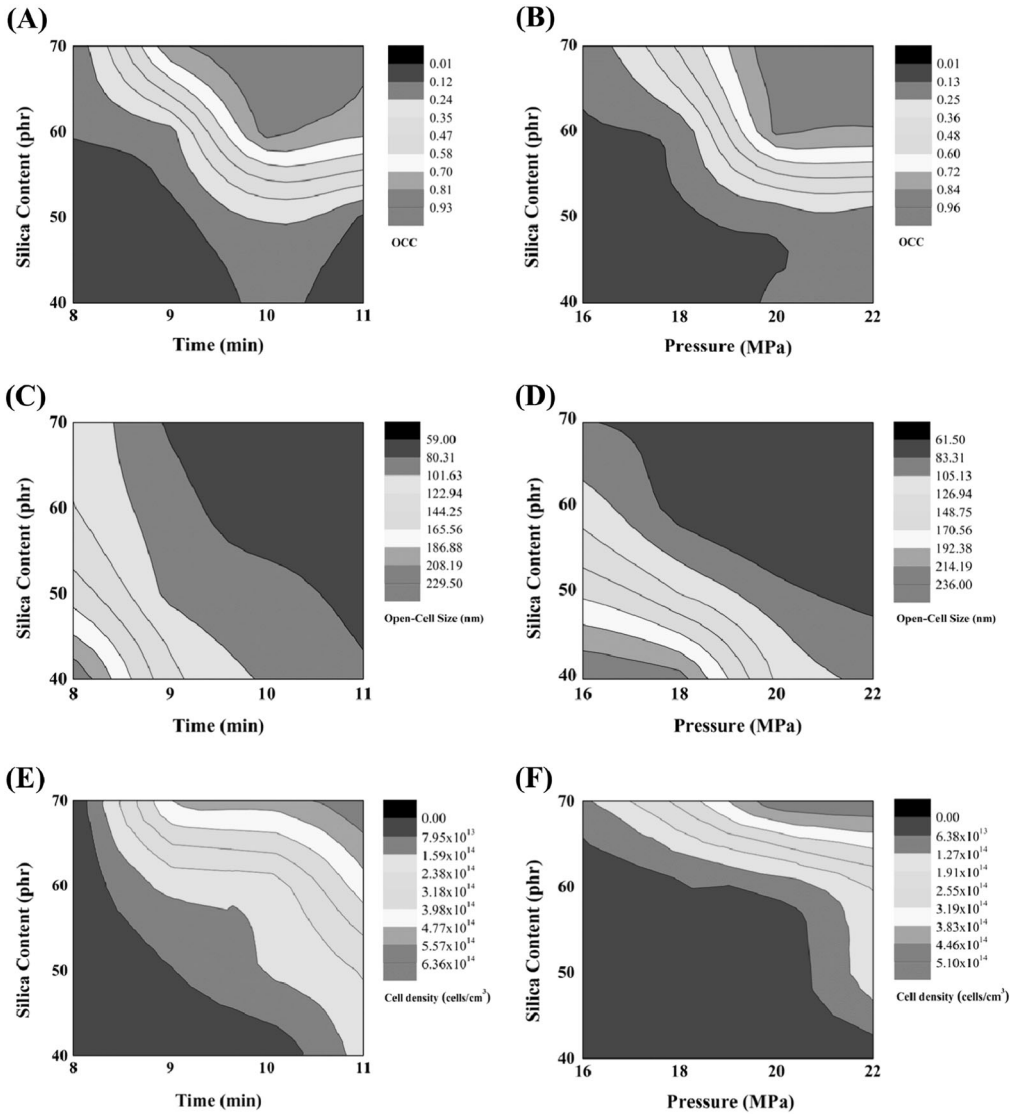

Fig. 6 The contour plot diagram of the OCC, cell diameter, and cell density of the nanocellular silicone rubber foams: **a** the effect of t_{pre} and silica content on the OCC; **b** the effect of *Ps* and silica content on the OCC; **c** the effect of t_{pre} and silica content on the open-cell size; **d** the effect of *Ps* and silica content on the open-cell size; **e** the effect of t_{pre} and silica content on the cell density; **f** the effect of *Ps* and silica content on the cell density

region gradually decreases. The reason for this result is the same as above. However, with a decrease in the cell size, the cellular compression shape decreases gradually, leading to a reduction in the width of the plateau. Finally, with an increase in the $scCO_2$ saturation temperature, the compression strength of the nano/micro silicone rubber foams decreases. This result is because the increase in the cell size caused by the $scCO_2$ saturation temperature reduces the bending resistance of the cell wall, resulting in the reduction of the height of the compression plateau. Figure 8 shows the effect of the OCC on the compressive properties of the nano/micro silicone rubber foams.

As shown in Fig. 8, one can see that there are two notable features. First, the compressive stress of the silicone rubber foams is approximately 0.7 MPa regardless of the value of the OCC. Second, when the OCC is less than 0.45%, the curves of the compressive measure can be divided into three regions. However, when the OCC is greater than 87%, the curve of the compressive measure displays two regions, namely, the linear elastic region and the densification region. The thickness of cell walls and the cellular structure are known to play important roles in the compressive property. On the one hand, thicker cell walls result in a more obvious plateau region. On the other hand, compared with a larger cell, the microcellular structure foam has a stronger performance [33], which could improve the plateau region. Hence, at the low-OCC level, the higher stress supported by the cell walls and microcellular structure could improve the plateau region. With an increase in the OCC, the presence of cavitation on cell walls causes a

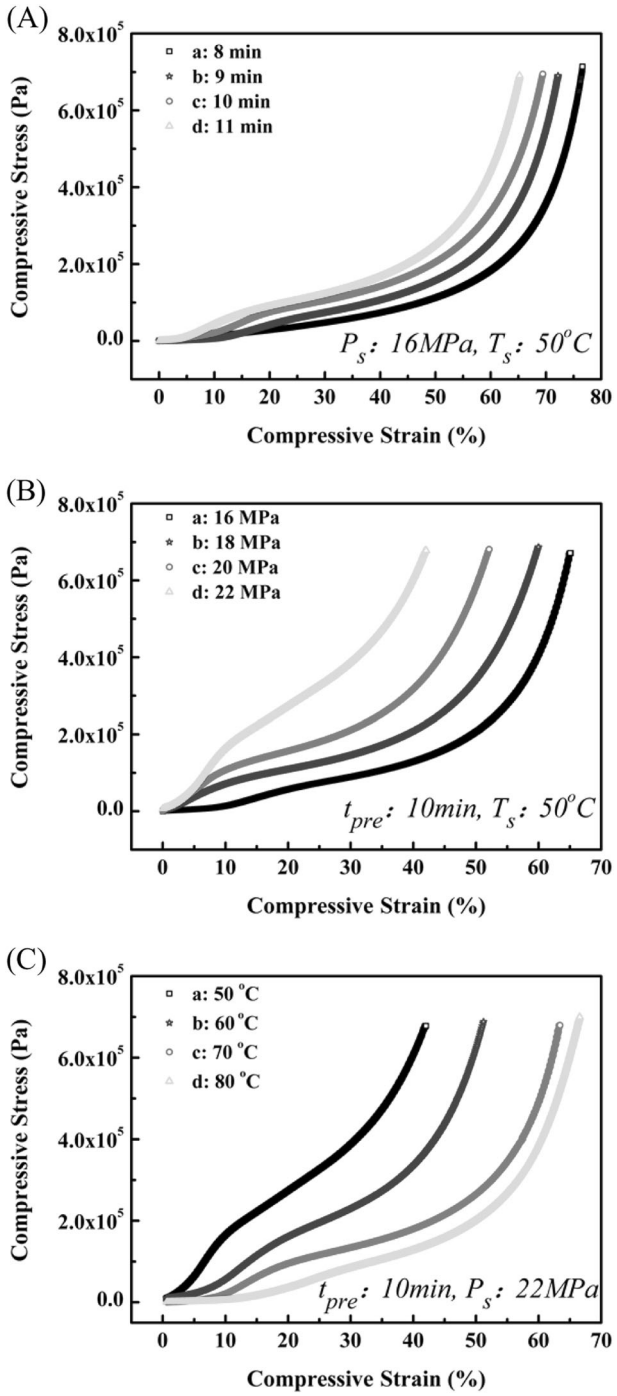

Fig. 7 Effect of the foaming parameters on the compressive property of the nano/micro silicone rubber foams. **a** t_{pre}, **b** *Ps*, **c** *Ts*

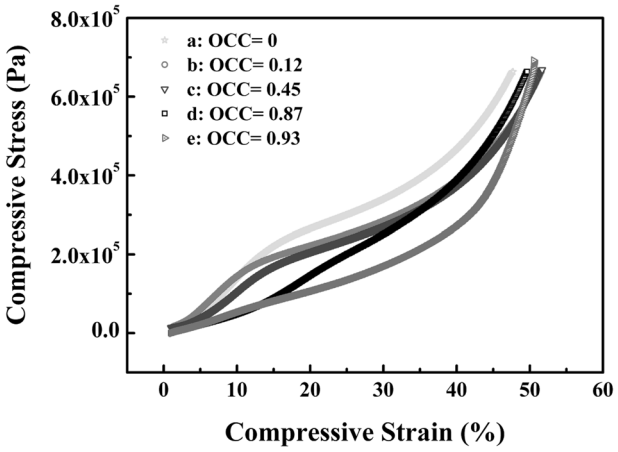

Fig. 8 Effect of the OCC on the compressive stress of the nano/micro silicone rubber foams

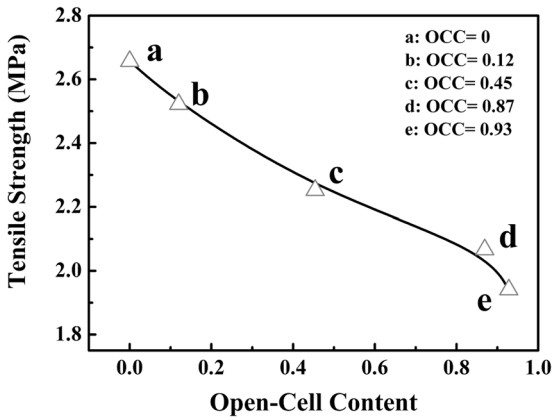

Fig. 9 Effect of the OCC on the tensile strength of the nano/micro silicone rubber foams

decrease in the stress supported by the cell walls, resulting in a decrease in the plateau region. When the OCC is greater than 87%, the stress supported by cell walls is very low because of a large amount of cavitation on the cell walls, resulting in the disappearance of the plateau region.

Figure 9 shows the influence of the OCC on the tensile strength of the nano/micro silicone rubber foams. The tensile strength of the silicone rubber foams decreases from 2.66 to 1.94 MPa when the OCC increases from 0 to 93%. On the one hand, the strength of the cell wall will decrease because of the presence of cavitation on the cell wall. Furthermore, greater cavitation weakens the strength of the cell wall. On the other hand, the thickness of the cell wall decreases with an increase in the OCC. The thickness of the cell wall decreases from approximately 2.31 to 0.57 μm when the cellular morphology changes from a microcellular structure to a nanocellular structure. Hence, the two factors cause an early breakdown in the tensile process, resulting in a decrease in the tensile strength. The same result has also been observed in PMMA nanocellular foams [34].

Conclusions

Microcellular and nanocellular silicone rubber foam prepared by $scCO_2$ is first reported in this work. The influence

of the cellular structure on the mechanical properties is presented. The minimum cell diameter and maximum cell density of the microcellular silicone rubber foam can reach 1.09 μm and 2.83×10^{11} cells/cm^3, respectively. The minimum value of the cell diameter and maximum value of the cell density of nanocellular silicone rubber foams can reach approximately 59 nm and 6.35×10^{14} cells/cm^3 when the silica content, t_{pre} and P_s are 70 wt%, 11 min, and 22 MPa. The nanocellular structure occurring on the cell walls could be attributed to stretching-induced cavitation. There are two factors affecting the formation of nanocellular structure. On the one hand, a large swelling ratio or high cell growth rate can increase the strain energy leading to the appearance of the nanocellular structure on the cell walls. The influence of the cellular morphology on the mechanical properties is investigated. When the cell is a continuous honeycomb structure and the cell size range is 1–3 μm, the compressive stress–strain curve of the nano/micro silicone rubber foams exhibits a high and wide compressive stress plateau region. The OCC has a significant effect on the compression plateau of the nano/micro silicone rubber foam. When the OCC increases, the presence of the cavitation on cell walls decreases the stress supported by the cell walls resulting in the gradual disappearance of the compression plateau. Furthermore, the tensile strength of the silicone rubber foams decreases from 2.66 to 1.94 MPa when the OCC increases from 0 to 93%.

Acknowledgements The authors acknowledge the financial support from the National Natural Science Foundation of China (Grant numbers: 51773186 and 51503189) and the Science and Technology Foundation of Institute of Chemical Materials (Grant number: KJCX-201402).

Compliance with ethical standards

Conflict of interest We declare that we have no financial and personal relationships with other people or organizations that can inappropriately influence our work, there is no professional or other personal interest of any nature or kind in any product, service and/or company that could be construed as influencing the position presented in, or the review of, the manuscript entitled, "Mechanical properties of the microcellular and nanocellular silicone rubber foams obtained by supercritical carbon dioxide".

References

1. Zhang A, Zhang Q, Bai H, Li L, Li J. Polymeric nanoporous materials fabricated with supercritical CO_2 and CO_2-expanded liquids. Chem Soc Rev. 2014;43:6938–53.
2. Costeux S. CO_2-blown nanocellular foams. J Appl Polym Sci. 2014;131:1–16.
3. Forest C, Chaumont P, Cassagnau P, Swoboda B, Sonntag P. Polymer nano-foams for insulating applications prepared from CO_2 foaming. Prog Polym Sci. 2015;41:122–45.
4. Realinho V, Antunes M, Martínez AB, Velasco JI. Influence of nanoclay concentration on the CO_2 diffusion and physical properties of PMMA montmorillonite microcellular foams. Ind Eng Chem Res. 2011;50:13819–24.
5. Zhai W, Yu J, Wu L, Ma W, He J. Heterogeneous nucleation uniformizing cell size distribution in microcellular nanocomposites foams. Polymer. 2006;47:7580–9.
6. Siripurapu S, De Simone JM, Khan SA, Spontak RJ. Controlled foaming of polymer films through restricted surface diffusion and the addition of nanosilica particles or CO_2-philic surfactants. Macromolecules. 2005;38:2271–80.
7. Yokoyama H, Sugiyama K. Nanocellular structures in block copolymers with CO_2-philic blocks using CO_2 as a blowing agent: crossover from micro- to nanocellular structures with depressurization temperature. Macromolecules. 2005;38:10516–22.
8. Taki K, Waratani Y, Ohshima M. Preparation of nanowells on a PS-b-PMMA copolymer thin film by CO_2 treatment. Macromol Mater Eng. 2008;293:589–97.
9. Ruiz JAR, Cloutet E, Dumon M. Investigation of the nanocellular foaming of polystyrene in supercritical CO_2 by adding a CO_2-philic perfluorinated block copolymer. J Appl Polym Sci. 2012;126:38–45.
10. Liu B, Wang P-C, Ao Y-Y, Zhao Y, An Y, Chen H-B, et al. Effects of combined neutron and gamma irradiation upon silicone foam. Radiat Phys Chem. 2017;133:31–6.
11. Yue Y, Zhang H, Zhang Z, Chen Y. Polymer–filler interaction of fumed silica filled polydimethylsiloxane investigated by bound rubber. Compos Sci Technol. 2013;86:1–8.
12. Wen J, Li Y, Zuo Y, Zhou G, Li J, Jiang L, et al. Preparation and characterization of nano-hydroxyapatite/silicone rubber composite. Mater Lett. 2008;62:3307–9.
13. Landrock AH. Glossary - Handbook of plastic foams, Manufacture and Applications (Elsevier, Technology & Engineering, Park Ridge), 456–481 (1995).
14. Chen H-B, Liu B, Huang W, Wu W-H. Gamma radiation induced effects of compressed silicone foam. Polym Degrad Stab. 2015;114:89–93.
15. Fang H, Li J, Chen H, Liu B, Huang W, Liu Y, et al. Radiation induced degradation of silica reinforced silicone foam: experiments and modeling. Mech Mater. 2017;105:148–56.
16. Liu P, Liu D, Zou H, Fan P, Xu W. Structure and properties of closed-cell foam prepared from irradiation crosslinked silicone rubber. J Appl Polym Sci. 2009;113:3590–5.
17. Grande JB, Fawcett AS, Mclaughlin AJ, Gonzaga F, Bender TP, Brook MA. Anhydrous formation of foamed silicone elastomers using the Piers–Rubinsztajn reaction. Polymer. 2012;53:3135–42.
18. Hong I-K, Lee S. Microcellular foaming of silicone rubber with supercritical carbon dioxide. Korean J Chem Eng. 2013;31:166–71.
19. Song L, Lu A, Feng P, Lu Z. Preparation of silicone rubber foam using supercritical carbon dioxide. Mater Lett. 2014;121:126–8.
20. Liao X, Xu H, Li S, Zhou C, Li G, Park CB. The effects of viscoelastic properties on the cellular morphology of silicone rubber foams generated by supercritical carbon dioxide. RSC Adv. 2015;5:106981–8.
21. Xu H, He Y, Liao X, Luo T, Li G, Yang Q, et al. A green and structure-controlled approach to the generation of silicone rubber foams by means of carbon dioxide. Cell Polym. 2016;35:19–32.
22. Yan H, Wang K, Zhao Y. Fabrication of silicone rubber foam with tailored porous structures by supercritical CO_2. Macromol Mater Eng. 2016;302:1600377.

23. Yang Q, Yu H, Song L, Lei Y, Zhang F, Lu A, et al. Solid-state microcellular high temperature vulcanized (HTV) silicone rubber foam with carbon dioxide. J Appl Polym Sci. 2017;134:44807.
24. Chandra A, Gong S, Yuan M, Turng LS, Gramann P, Cordes H. Microstructure and crystallography in microcellular injection-molded polyamide-6 nanocomposite and neat resin. Polym Eng Sci. 2005;45:52–61.
25. Yang J, Huang L, Zhang Y, Chen F, Fan P, Zhong M, et al. Nucleating agent for polymer foaming: applications of ordered mesoporous silica particles in polymethyl methacrylate supercritical carbon dioxide microcellular foaming. Ind Eng Chem Res. 2013;52:14169–78.
26. Sheng SJ, Hu X, Wang F, Ma QY, Gu MF. Mechanical and thermal property characterization of poly-l-lactide (PLLA) scaffold developed using pressure-controllable green foaming technology. Mater Sci Eng C. 2015;49:612.
27. Yu P, Mi HY, Huang A, Geng LH, Chen BY, Kuang TR. et al. Effect of poly(butylenes succinate) on poly(lactic acid) foaming behavior: formation of open cell structure. Ind Eng Chem Res. 2015;54:6199–6207.
28. Zhou C, Vaccaro N, Sundarram SS, Li W. Fabrication and characterization of polyetherimide nanofoams using supercritical CO_2. J Cell Plast. 2015;48:239–55.
29. Guo H, Nicolae A, Kumar V. Solid-state microcellular and nanocellular polysulfone foams. J Polym Sci Part B: Polym Phys. 2015;53:975–85.
30. Gong P, Taniguchi T, Ohshima M. Nanoporous structure of the cell walls of polycarbonate foams. J Mater Sci. 2014;49:2605–17.
31. Guo H, Nicolae A, Kumar V. Solid-state microcellular and nanocellular polysulfone foams. J Polym Sci Part B: Polym Phys. 2015;53:975–85.
32. Gibson LJ, Ashby MF. Cellular solids: structure and properties. Cambridge, UK: Cambridge University Press; 1997.
33. Ma Z, Zhang G, Yang Q, Shi X, Liu Y. Mechanical and dielectric properties of microcellular polycarbonate foams with unimodal or bimodal cell-size distributions. J Cell Plast. 2014;51:307–27.
34. Notario B, Pinto J, Rodríguez-Pérez MA. Towards a new generation of polymeric foams: PMMA nanocellular foams with enhanced physical properties. Polymer. 2015;63:116–26.